and E. Haselbach, *J. Am. Chem. Soc.*, **98**, 5428 (1976); (c) J. D. Dill, P. v. R. Schleyer, and J. A. Pople, *ibid.*, **99**, 1 (1977).
(9) R. W. Taft, *J. Am. Chem. Soc.*, **83**, 3350 (1961).
(10) R. A. Abramovich and G. Tertzakian, *Can. J. Chem.*, **43**, 940 (1965); R. A. Abramovitch and J. G. Saha, *ibid.*, **43**, 3269 (1965).
(11) N. Kamigata, M. Kobayashi, and H. Minato, *Bull. Chem. Soc. Jpn.*, **45**, 2047 (1972).
(12) A. Cox, T. J. Kemp, D. R. Payne, M. C. R. Symons, D. M. Allen, and P. Pinot de Moira, *J. Chem. Soc., Chem. Commun.*, 693 (1976).
(13) H. Böttcher, H. G. O. Becker, V. L. Ivanov, and M. G. Kuzmin, *Chimia*, **27**, 437 (1973).
(14) E. Wasserman, L. C. Snyder, and W. A. Yager, *J. Chem. Phys.*, **41**, 1763 (1964).
(15) E. Wasserman and R. W. Murray, *J. Am. Chem. Soc.*, **86**, 4203 (1964).

An Electron Spin Resonance Study of the Association of a Surfactant Nitroxyl Radical with a Cationic Micelle Using Spin-Intensity Measurements and Hyperfine Structure Analyses

C. L. Kwan, Samir Atik, and Lawrence A. Singer*

Contribution from the Department of Chemistry, University of Southern California, Los Angeles, California 90007. *Received August 3, 1977*

Abstract: The association constant, $K = (3.2 \pm 0.2) \times 10^5\ M^{-1}$, for incorporation of 4-[*N*,*N*-dimethyl-*N*-(*n*-hexadecyl)ammonium]-2,2,6,6-tetramethylpiperidinyl-*N*-oxy chloride (**1**) into the hexadecyltrimethylammonium chloride micelle was determined from analyses of composite spectra made up of free **1** and singly bound **1** and spin-intensity measurements. The hyperfine structure observed in the ESR spectrum of free **1** in water is lost upon binding with the micelle. The severe line broadening (5–10 G) in the spectrum of **1** located in multiply occupied micelles leads to apparent intensity loss in peak to peak measurements of the unbroadened 1.7-G middle-field line of **1** from both free and singly bound **1**. The data are analyzed in terms of a multiple-step equilibrium model for the incorporation of **1**, which provides a critical micelle concentration of 4×10^{-3} M and a number-average aggregation number of 59 ± 7 for the hexadecyltrimethylammonium chloride micelle.

Introduction

Nitroxyl radicals have been widely used for a number of years for studying the properties and reactivities of assemblies such as bilayers and micelles.[1] We describe an ESR method, based on the measurements of both signal intensity and change in hyperfine structure, for studying the association of surfactant nitroxyl radicals with micelles.

Most previous studies that qualitatively[2] and quantitatively[3] studied the association of nitroxyl radicals with micelles were based on the difference in field position observed for the high-field line of the bound and free nitroxyl radicals. This approach is limited to cases where the resulting field shift, due to changes in *g* values and nitrogen splitting for the bound and free spin labels, is large enough to be distinguished.

Our approach, which does not have this limitation, provides the *K* for association of the nitroxyl radical with the micelle structure, as well as association information on the micelle itself (critical micelle concentration, i.e., CMC, and aggregation number). This methodology is demonstrated with the surfactant nitroxyl radical **1**/hexadecyltrimethylammonium

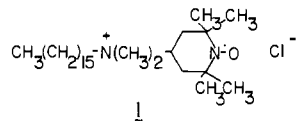

1

chloride (more commonly called cetyltrimethylammonium chloride or "CTAC") system. Further, we analyzed the ESR data in terms of a multiple-step equilibrium model for incorporating the spin label into the micelle structure.[4]

Results and Discussion

4-[*N*,*N*-Dimethyl-*N*-(*n* - hexadecyl)ammonium] - 2,2,-6,6-tetramethylpiperidinyl-*N*-oxy chloride (**1**) was prepared by conventional procedures as described in the Experimental Section.

In pure water at $\sim 10^{-5}$ M, **1** shows the typical three-line nitrogen-splitting pattern (a_N = 16.9 G) of nitroxyl radicals. Degassed solutions reveal hydrogen hyperfine structure (~0.5 G)[5] which is particularly noticeable in the low- and middle-field lines. (Figure 1). Although these hyperfine structures were previously reported,[6] they have not been used for diagnostic purposes.

We find these structures to be sensitive to the microenvironment of **1**. Figure 2, series A, shows representative spectra of the middle-field line. The top spectrum was recorded in pure water, while the bottom spectrum was observed in the presence of 4.0×10^{-2} M CTAC. The latter is well above the CMC point of CTAC, generally estimated to be $\sim 1.0 \times 10^{-3}$ M.[7] We assume that the bottom spectrum in series A corresponds to **1** singly bound to the CTAC micelle.[8] The loss of the hydrogen hyperfine structure for singly bound **1** may be associated with a slower tumbling rate for **1** in the micelle environment.[2,9]

As pointed out by Oakes,[2a] above the CMC point the ESR spectrum of a nitroxyl radical usually is a superposition of two individual spectra weighted according to the respective concentrations of the aqueous and micellar states.[10] Indeed, a series of spectra in the range $5\text{–}7 \times 10^{-3}$ M CTAC could be computer simulated as a composite of the free (top) and bound (bottom) states of **1**; see Figure 2. Figure 2, series B, shows representative simulated spectra for two intermediate CTAC concentrations. Note that this matchup between the experimental and simulated spectra is based on the details in the hyperfine structure in addition to the slight differences in *g* and a_N values of nitroxyl radicals in aqueous and micellar environments as used by previous studies.[3] Further, our approach is not jeopardized by the superposition of a severely broadened ($\gtrsim$5 G) spectrum of **1** in multiply occupied micelles which is described below.

Since the composite spectra could be simulated using the line width of **1** in pure water, we estimate the broadening of free

0002-7863/78/1500-4783$01.00/0

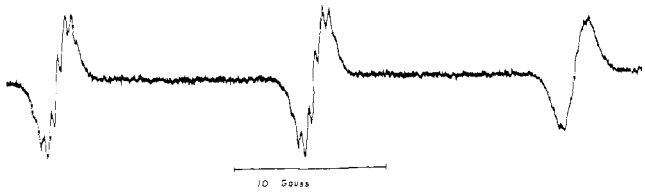

Figure 1. ESR spectrum of 4.0×10^{-5} M **1** in water at 25 °C. Modulation amplitude 0.1 G.

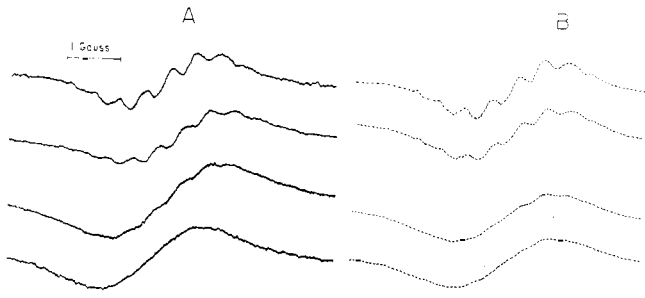

Figure 2. Comparison of experimental (series A) and simulated (series B) spectra of the middle-field line of 4.0×10^{-5} M **1**. Series A at [CTAC] of (top to bottom): 0, 5.0×10^{-3}, 6.4×10^{-3}, and 4.0×10^{-2} M. Series B for fraction of monomeric bound **1** (top to bottom): 0, 0.50, 0.85 and 1.00. Modulation amplitude 0.1 G.

1 in the presence of micelles, due to exchange of **1** between the aqueous and micellar environments, is $\lesssim$0.1 G, which indicates an exchange frequency $<3 \times 10^5$ Hz.[11]

In the presence of 5×10^{-3} M CTAC, under conditions of high modulation amplitude, the broad-field spectrum of **1** clearly reveals the presence of a broadened spectrum in addition to the narrower (1.7 G) composite spectra as shown in Figure 4. We assume this severe broadening results from spin exchange[2b] (vide infra) between nitroxyl radicals incorporated into the same micelle.[12] Thus, while the spectrum of **1** in singly occupied micelles only shows loss of hyperfine structure compared to free **1**, the spectrum of **1** in multiply occupied micelles is broadened to $\gtrsim$5.0 G, *which leads to apparent intensity loss in peak to peak measurements on the 1.7-G middle-field line.*[13]

Figure 3, upper, shows the results of these intensity measurements. The intensity loss is most pronounced near 5×10^{-3} M CTAC (Figure 4) where the normalized intensity corresponds to only 30% of that in pure water. This minimum occurs just above our estimate of the CTAC CMC point (see discussion below). Thereafter, the intensity increases again and returns completely near 0.05 M CTAC (Figure 4).

The onset of intensity loss with added CTAC below the CMC point suggests that **1** is associating with submicellar aggregates of CTAC.[14] The maximum intensity loss appears just after micellization when **1** is clustered among the few available micelles. The intensity return with added CTAC above the CMC point is understandable, since **1** is increasingly dispersed among the growing number of micelles.[15]

The lower part of Figure 3 is a plot of the ratio of bound **1** [N_b] to free **1** [N] vs. added surfactant. The $[N_b]/[N]$ values were determined as follows. $[N_b] = [M{\cdot}N] + 2[M{\cdot}N_2] \ldots + n[M{\cdot}N_n]$, where $[M{\cdot}N_n]$ is the concentration of micelles with n nitroxyl radicals. If we assume the intensity loss is due to all $M{\cdot}N_n$, where $n > 1$,[12] the total concentration of monomeric **1** (bound and free) is given by

$$[M{\cdot}N] + [N] = I_r[N_T] \qquad (1)$$

where I_r is the normalized relative intensity. The $[M{\cdot}N]/[N]$ values are available from the simulated spectra (Figure 2B). Thus, from the intensity measurements and simulations, we determined [N], $[M{\cdot}N]$ and $\Sigma_n[M{\cdot}N_n]$ where $n > 1$.

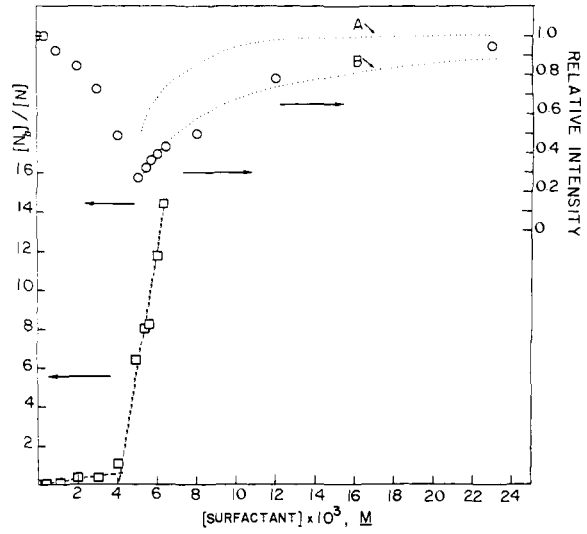

Figure 3. Effect of added CTAC on the middle-field line ESR spectrum of **1**. (○) Normalized relative intensity. (□) Ratio of [total bound **1**] to [free **1**]. (. . .) simulated normalized relative intensity profiles for intensity loss due to $[M{\cdot}N_n]$ where (A) $n \leq 2$ and (B) $n = 1$.

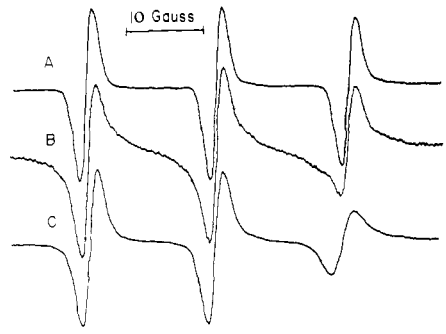

Figure 4. ESR spectrum of 4.0×10^{-5} M **1** in (A) pure water, in the (B) presence of 5.0×10^{-3} M CTAC, and in the (C) presence of 4.0×10^{-2} M CTAC. Modulation amplitude 1.0 G.

Analysis of the Data. From the $[N_b]/[N]$ data in Figure 3, we place the CMC point of CTAC near 4×10^{-3} M[16] which is the origin of the sharp discontinuity in the $[N_b]/[N]$ values. Also at this concentration of CTAC, the loss of signal intensity accelerates, suggesting again that it is a point of discontinuity.

The intensity loss below the CMC point apparently results from the aggregation of **1** in premicellar structures of CTAC. The determination of the usefulness of ESR intensity measurements for the quantitative study of this premicellar state is outside the scope of the present investigation.

Above the apparent CMC point, the data is consistent with a stepwise incorporation of **1** into the micellar structure by the scheme shown below.

$$M + N \underset{k'}{\overset{k}{\rightleftharpoons}} M{\cdot}N \qquad (2)$$

$$M{\cdot}N + N \underset{2k'}{\overset{k}{\rightleftharpoons}} M{\cdot}N_2 \qquad (3)$$

$$\vdots \qquad\qquad \vdots$$

$$M{\cdot}N_{n-1} + N \underset{nk'}{\overset{k}{\rightleftharpoons}} M{\cdot}N_n \qquad (4)$$

In this scheme, it is assumed that the rate constant for association of N into the micelle is k at each step, while the dis-

sociation rate constant is nk'. The equilibrium constant for each step is

$$K_n = [M{\cdot}N_n]/\{[M{\cdot}N_{n-1}][N]\} \quad (5)$$

where $K_n = k/nk' = K/n$.

The total concentration of **1** is

$$[N_T] = [N] + \sum_{n=1}^{\infty} n[M{\cdot}N_n]. \quad (6)$$

Based on the relationships in eq 5,

$$[N_T] = [N] + [M]K[N] + [M](K[N])^2 + 0.5[M](K[N])^3 \cdots \frac{1}{[n-1]!}[M](K[N])^n \quad (7)$$

which can be rewritten as

$$[N_T] = [N] + [M]K[N]\{1 + (K[N]) + 0.5(K[N])^2 \cdots [1/(n-1)!](K[N])^{n-1}\} \quad (8)$$

Noting that the second term in the above is a Taylor series expansion, it follows that:

$$[N_T] = [N] + [M]K[N]e^{K[N]} \quad (9)$$

where the total concentration of bound **1** is

$$[N_b] = [M]K[N]e^{K[N]} \quad (10)$$

Similarly, the total micelle concentration is expressed as

$$[M_T] = [M]e^{K[N]} \quad (11)$$

From eq 10 and 11,

$$[N_b]/[N] = K[M_T] \quad (12)$$

Ignoring any premicellar aggregates, the total concentration of micelles is related to the CMC by

$$[M_T] = \{[CTAC] - [CMC]\}/n' \quad (13)$$

where n' is the aggregation number. Thus,

$$[N_b]/[N] = K\{[CTAC] - [CMC]\}/n' \quad (14)$$

Equation 14 predicts a linear plot for $[N_b]/[N]$ vs. [CTAC] with an x axis intercept of [CTAC] = [CMC]. The lower portion of Figure 3 shows this plot which provides [CMC] $\simeq 4 \times 10^{-3}$ M[16] and a slope of $K/n' = (5.4 \pm 0.3) \times 10^3$ M^{-1}.

From eq 5 with $n = 1$ and eq 10

$$[N_b]/[M{\cdot}N] = e^{K[N]} \quad (15)$$

which predicts that a plot of ln $\{[N_b]/[M{\cdot}N]\}$ vs. [N] should be linear with a slope of K. This plot in Figure 5 provides $K = (3.2 \pm 0.2) \times 10^5$ M^{-1}. Using this K with the slope of Figure 3, lower, gives $n' = 59 \pm 7$.

The $K \simeq 3 \times 10^5$ M^{-1} for the incorporation of **1** into the CTAC micelle is comparable in magnitude to $K = 7.00 \times 10^5$ M^{-1} for incorporation of **2** into the hexadecyltrimethylammonium bromide micelle.[17] This latter value was indirectly determined by a kinetic study of the hydrolysis of **2** under micellar conditions.

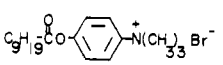

2

The $n' = 59 \pm 7$[18] determined in this study for the CTAC micelle is a number-average (N_n) aggregation number. Others[14b] have pointed out that different estimates of aggregation number are obtained by different methods of investigation depending on whether the result is a weight average (N_w) or N_n. This difference between N_n and N_w occurs when the micelle system is polydispersed, meaning that a range of micelles of varying size is present. For polydispersed micelles, $N_w > N_n$.

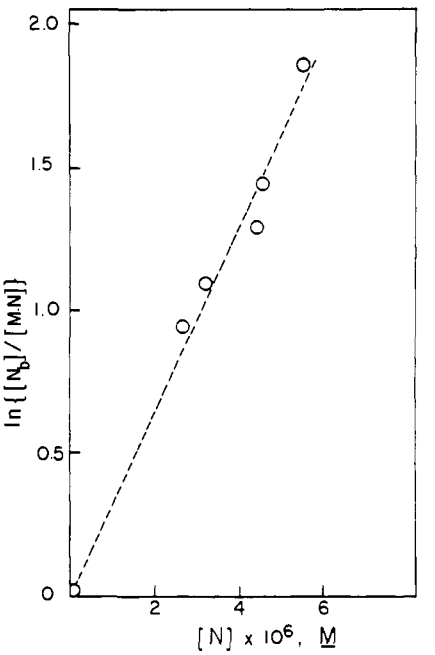

Figure 5. Plot of ln [(total bound **1**)/(monomeric bound **1**)] vs. free **1**.

Self-consistency of the Data. The assumption stated earlier that the intensity loss in peak to peak measurements is associated with all micelles containing *two or more* spin probes can be examined. The *unbroadened* signal intensity provides a measure of [N] (i.e., free **1**) and [N_b'] (i.e., all the bound **1** having unbroadened lines and where the spin-probe occupancy level is not yet specified). The portion of the narrow line intensity due to [N] is determined by the previously described analysis of the composite spectra with the assumption that the observed narrow-line spectra are a weighted linear combination of two individual spectra due to [N] and [N_b']. The concentration of *all* bound **1** (i.e., the bound **1** having either narrow or broadened lines) is $[N_b] = [N_T] - [N]$. The relative populations of $\{[M{\cdot}N], [M{\cdot}N_2] \ldots [M{\cdot}N_n]\}$ that comprise $[N_b]$ are determined by the Poisson distribution function.[19]

$$P_n = (X^n/n!)e^{-X} \quad (16)$$

where $X = [N_b]/[M_T]$ with $[M_T]$ being determined from eq 13 using our values for [CMC] and n'.

In Figure 3 are shown the calculated relative intensity curves for the two cases where the observed (unbroadened) intensity is due to contributions from (A) + [N] + $[M{\cdot}N]$ + $[M{\cdot}N_2]$ or (B) [N] + $[M{\cdot}N]$. Case B is within experimental error of the measured intensities while A is not, indicating that there are no significant peak to peak intensity contributions from $[M{\cdot}N_n]$ when $n \geq 2$.

In summary, computer simulations, based on the differences in the hyperfine structure in the ESR spectra of nitroxyl radicals, were used to follow binding of the latter to micelles. The measurements of spin-intensity loss, due to aggregates $M{\cdot}N_2$ and higher, and the computer simulations were analyzed using a multiple-step equilibrium model for nitroxyl-radical binding to the micelle. This approach provides the K for association as well as the CMC point and number-average aggregation number of the micelle.

Experimental Section

Syntheses. 4-(*N,N*-Dimethylamino)-2,2,6,6-tetramethylpiperidine (2) was prepared by the method of Icke and Wisegarver.[20] To 25.5 g

(0.5 mol) of 90% formic acid cooled in an ice bath was added with stirring 15.6 g (0.1 mol) of 4-amino-2,2,6,6-tetramethylpiperidine (Aldrich Chemical Co.) followed by 17.8 g (0.22 mol) of 37% aqueous formaldehyde solution. The mixture was then refluxed for 8 h, 11 g of concentrated hydrochloric acid was added, and the formic acid and excess formaldehyde were removed under reduced pressure. The oily orange residue was dissolved in 75 mL of water and 30 g of solid sodium hydroxide was added. The orange upper layer was collected and the lower aqueous layer was extracted twice with 50 mL of diethyl ether. The combined extracts were added to the upper layer and dried over potassium hydroxide pellets. The ether was removed in vacuo and the residue was vacuum distilled [32 °C (0.1 mm)] to give a colorless liquid (70%).

4-[*N,N*-Dimethyl-*N*-(*n*-hexadecyl)ammonium]-2,2,6,6-tetramethylpiperidinyl Bromide (3). To 2.4 g (0.013 mol) of **2** was added 4.6 g (0.015 mol) of *n*-hexadecyl bromide. The mixture was heated in an oil bath at 75 °C for 12 h. The cooled glassy residue was triturated several times with petroleum ether to give a fine white granular solid (mp 77–80 °C).

4-[*N,N*-Dimethyl-*N*-(*n*-hexadecyl)ammonium]-2,2,6,6-tetramethylpiperidinyl-*N*-oxy chloride (1) was prepared by the oxidation procedure described by Rozantsev.[21] To a mixture of 0.15 g of disodium ethylenediaminetetraacetate dihydrate and 0.15 g of sodium hydrogen tungstate in 20 mL of water was added 4.9 g (0.010 mol) of **3** in 20 mL of methanol. The resulting mixture was cooled in an ice bath and 2.5 mL of 30% hydrogen peroxide was added with stirring. The mixture was stirred at room temperature for 10 days. The final orange solution was extracted twice with 50 mL of dichloromethane. The extracts were combined and concentrated in vacuo to give an orange solid residue which was triturated several times with petroleum ether. The product was recrystallized three times from dichloromethane–petroleum ether, yielding an orange powder: mp 134–135 °C; UV-vis λ_{max} 450 nm, ϵ 10.

Anal. Calcd for $C_{27}H_{56}N_2OBr$: C, 64.28; H, 11.11; N, 5.56. Found: C, 63.55; H, 11.08; N, 5.43.

The chloride salt was prepared by passing an aqueous solution of the bromide salt through an Amberlite, IRA-400, ion-exchange column.

ESR Measurements. All spectra were recorded on a Varian E-12 X-band spectrometer equipped with a V-4532 dual sample cavity operated in the TE 102 mode with a resonance frequency near 9.5 GHz and a modulation frequency of 100 kHz. The sample tubes were 100-μL disposable micropipets manufactured by Corning Glass Corp. (no. 7099S). Using these sample tubes, we obtained tube to tube reproducible signal intensity of ±5%. The samples of **1** in the concentration range (4–7) × 10^{-3} M CTAC were degassed by the freeze–pump–thaw method in order to better resolve the hyperfine structure of free **1**.

The intensity measurements were made relative to standard aqueous solutions of 4-carboxyl-2,2,6,6-tetramethylpiperidinyl-*N*-oxy[22] in the second channel of the dual cavity. Identical microwave power, crystal biasing current, field-scanning rate, and modulation amplitude were used in each cavity. The sample/standard dual-cavity spectra were recorded twice in the A channel/B channel and B channel/A channel configurations, and the data were analyzed using the double-integration method as suggested by Ayscough.[23] The intensity measurements with and without the dual-cavity technique agreed within 5%, suggesting little or no perturbation of the cavity Q by the small sample cells and low concentrations used.

Computer Simulations. The simulated spectra were obtained by digitizing the normalized spectra of the free (S_N) and bound ($S_{M\cdot N}$) **1** (top and bottom spectra, Figure 2A) and recombining them according to

$$S_C = f(S_N) + (1 - f)(S_{M\cdot N})$$

where S_C is the composite spectrum and f is the fraction of free **1**.

References and Notes

(1) (a) L. J. Berliner, Ed., "Spin Labeling. Theory and Applications", Academic Press, New York, N.Y., 1976. (b) J. H. Fendler and E. J. Fendler, "Catalysis in Micellar and Macromolecular Systems", Academic Press, New York, N.Y., 1975.

(2) (a) J. Oakes, *Nature (London)*, **231**, 38 (1971). (b) O. H. Griffith and A. S. Waggoner, *Acc. Chem. Res.*, **2**, 17 (1969), and references therein.

(3) N. M. Atherton and S. J. Strach, *J. Chem. Soc., Faraday Trans. 2*, **68**, 374 (1974). The slight difference between g and a_N values for 1 in an aqueous or micellar environment shifts the symmetry of the composite spectra. This shift, which was observed in our experimental spectra, cannot be explained by the modulation produced by movement of **1** into and out of the micellar environment.

(4) A similar model was used to describe quenching of the fluorescence from micelle-solubilized fluorophors by micelle-bound quenchers. M. Tachiya, *Chem. Phys. Lett.*, **33**, 289 (1975).

(5) K. K. Fox, *J. Chem. Soc., Faraday Trans. 2*, **72**, 975 (1976).

(6) (a) R. Kreilick, *J. Chem. Phys.*, **46**, 4260 (1967). (b) N. M. Atherton and S. J. Strach, *J. Magn. Reson.*, **17**, 134 (1975).

(7) P. Mukerjee and K. Mysels, "Critical Micelle Concentrations of Aqueous Surfactant Systems", National Standards Reference Data Series, National Bureau of Standards, Washington, D.C., 1971.

(8) At [CTAC] = 4.0 × 10^{-2} M, if the CMC = 1.0 × 10^{-2} M, which is well above literature estimates,[7] the micelle concentration is [M] = 3.0 × 10^{-4} M if the aggregation number is 100. At a total nitroxyl radical concentration of [N_T] = 4.0 × 10^{-5} M which is all micelle bound, 93.5% of **1** will be singly bound using the random Poisson distribution model (see later discussion in text). At CMC = 1.0 × 10^{-3} M, 95% of **1** is singly bound.

(9) G. Poggi and C. S. Johnson, Jr., *J. Magn. Reson.*, **3**, 436 (1970).

(10) We observe a distinct change of symmetry for the hyperfine structure in the concentration range 4–6 × 10^{-3} M CTAC which is consistent with a composite of two spectra with slightly different g values.[2a] This observation precludes the possibility of increased broadening of a single spectrum due to change in correlation time with added CTAC.

(11) K. K. Fox, *Trans. Faraday Soc.*, **67**, 2802 (1971), arrived at a similar estimate.

(12) We estimate the effective local concentration of **1** for a doubly occupied micelle to be 0.05–0.1 M assuming a radius of 20–25 Å and concentration relationship experimentally determined for 4-oxo-2,2,6,6-tetramethylpiperidinyl-*N*-oxy, this effective concentration should lead to a line width of ≳5 G, as is noted in Figure 4. A. D. Keith and W. Snipes *ACS Symp. Ser. n34*, 426 (1976).

(13) Based on a Lorentzian line shape, the peak to peak height of the first derivative spectrum varies with the inverse square of the width. The observed peak to peak intensity of a 1.7-G line (unbroadened) will be increased 5% by a line of similar g value having a width of 5.0 G, when both are of equal population and will also increased 2% by a line of 10-G width when the relative populations are 1:2.5, respectively. The latter very nearly corresponds to the 5.0 × 10^{-3} M CTAC case.

(14) Submicellar aggregates of variable size are proposed in the polydispersity, multiple-equilibrium model for surfactant association. For example, see (a) P. Mukerjee, *J. Pharm. Sci.*, **63**, 972 (1974); (b) L. R. Fisher and D. G. Oakenfull, *Chem. Soc. Rev.*, **6**, 25 (1977).

(15) The intensity variations are not due to probe self-association, since the concentration of **1** in these experiments was well below the point where self-aggregation occurs. We observe that in pure water the signal intensity of the middle-field line of **1** is within >90% of the theoretical maximum value and is directly proportional to [**1**] up to ~5 × 10^{-4} M. Above that point, the signal intensity/concentration profile levels off. Further, at ≳5 × 10^{-4} M a severely broadened (~15 G) single line appears which increases in intensity with added [**1**]. We assign the latter to micelle structures of **1** and estimate the CMC to be ~5 × 10^{-4} M.

(16) A similar CMC point for CTAC recently was estimated from fluorescence studies by M. W. Geiger and N. J. Turro, *Photochem. Photobiol.*, **22**, 273 (1975).

(17) T. C. Bruice, T. Katzhendler, and L. R. Fedor, *J. Am. Chem. Soc.*, **90**, 1333 (1968).

(18) The aggregation number of the hexadecyltrimethylammonium bromide micelle was recently given as 61 in reference 1b, p 21. However, values between 70 and 90 are often quoted. See reference 17 and references therein. From data given in reference 1b for other surfactants, the aggregation number does not seem to vary significantly with change in anion.

(19) R. C. Dorrance and T. F. Hunter, *J. Chem. Soc., Faraday Trans. 1*, **70**, 1572 (1974).

(20) R. N. Icke and B. B. Wisegarver, in "Organic Syntheses", Collect. Vol. III, Wiley, New York, N.Y. 1955, p 723.

(21) E. G. Rozantsev, "Free Nitroxyl Radicals", Plenum Press, New York, N.Y. 1970.

(22) E. J. Rauckman, G. M. Rosen, and M. B. Abou-Donia, *J. Org. Chem.*, **41**, 564 (1976).

(23) P. B. Ayscough, "Electron Spin Resonance in Chemistry", Methuen and Co., Ltd., London, 1967, p 165.